

Increased Protein Arginine Methylation in Chronic Hypoxia

Role of Protein Arginine Methyltransferases

Ali O. Yildirim, Patrick Bulau, Dariusz Zakrzewicz, Kamila E. Kitowska, Norbert Weissmann, Friedrich Grimminger, Rory E. Morty, and Oliver Eickelberg

Department of Medicine II, University of Giessen Lung Center, Justus-Liebig University Giessen, Giessen, Germany

Asymmetric dimethylarginine (ADMA) is an endogenous inhibitor of nitric oxide synthesis. ADMA is generated by catabolism of proteins containing methylated arginine residues, and its levels are correlated with endothelial dysfunction in systemic cardiovascular diseases. Arginine methylation of cellular proteins is catalyzed by protein arginine methyltransferases (PRMT). The expression and localization of PRMT in the lung has not been addressed. Here, we sought to analyze the expression of PRMT isoforms in the lung and to determine whether PRMT expression is altered during exposure to chronic hypoxia (10% oxygen). Adult mice were exposed to hypoxia for up to 3 wk, and lung tissues were harvested and processed for RT-PCR, Western blotting, immunohistochemistry, and determination of tissue ADMA levels. All PRMT isoforms investigated were detected at the mRNA and protein level in mouse lung, and were localized primarily to the bronchial and alveolar epithelium. In lungs of mice subjected to chronic hypoxia, PRMT2 mRNA and protein levels were up-regulated, whereas the expression of all other PRMT isoforms remained unchanged. This was mainly due to increased expression of PRMT2 in alveolar type II cells, which did not express detectable levels of PRMT2 under normoxic conditions. Consistent with these observations, lung ADMA levels and ADMA/L-Arginine ratios were increased under hypoxic conditions. These results demonstrate that PRMTs are expressed and functional in the lung, and that hypoxia is a potent regulator of PRMT2 expression and lung ADMA concentrations. These data suggest that structural and functional changes caused by hypoxia may be linked to ADMA metabolism.

Keywords: bronchial epithelium; immunohistochemistry; protein methylation; vessels

Hypoxia is a potent stimulus for lung vascular and interstitial remodeling during development, and in diseases such as chronic obstructive pulmonary disease (COPD), pulmonary hypertension, and asthma (1–3). Long-term (chronic) hypoxia modulates gene expression and thus can induce structural changes in the lung (4). These changes include increased fibroblast and vascular smooth muscle cell proliferation and enhanced deposition of extracellular matrix, resulting in sustained increases in pulmonary vascular resistance (4, 5). In the response to hypoxia, the release of short-lived mediators such as nitric oxide (NO) repre-

sents a key mechanism in the control of vascular resistance and vascular cell proliferation (6, 7). The role of NO production in the hypoxic lung, however, remains controversial. Several studies have shown decreased NO production during alveolar hypoxia, which may be due to O₂ substrate limitation, NO synthase (NOS) expression, or NOS activity, while other studies have shown the opposite (6). In recent years, our basic understanding of the control of NOS has advanced with the discovery of endogenous inhibitors of NOS, such as asymmetric dimethylarginine (ADMA) and N^G-monomethyl-L-arginine (L-NMMA). ADMA and L-NMMA both belong to the class of naturally occurring analogs of the NO precursor L-arginine, and act as endogenous inhibitors of all NOS isoforms (8, 9).

ADMA and L-NMMA are generated through degradation of cellular proteins that contain methylated arginine residues (10). It has been demonstrated that, during post-translational modification of many intracellular proteins, nitrogen atoms of arginine residues can be covalently mono- or di-methylated by the action of protein arginine methyltransferases (PRMT), a recently discovered gene family (11). Up to now, eight PRMT isoforms have been cloned and characterized in mammals, displaying varying degrees of substrate specificity (10–12). PRMTs catalyze the transfer of one or two methyl groups provided by S-adenosyl-methionine to select target proteins, either in symmetric configuration (leading to symmetric dimethylarginine [SDMA]), or in asymmetric configuration (leading to ADMA). PRMTs can be divided into two groups: type I PRMT catalyze ADMA formation in select target proteins, whereas type II PRMT catalyze SDMA formation through methylation of both guanidino nitrogens. In addition, all PRMT can also catalyze monomethylation, leading to the formation of L-NMMA. Free cellular ADMA and L-NMMA can be hydrolyzed by dimethylarginine dimethylaminohydrolases (DDAH) (10).

The biological impact of protein arginine methylation remains to be fully elucidated, but it has been shown to modify protein functions by regulating protein-protein interactions, both negatively and positively. Furthermore, arginine methylation in target proteins plays a role in the regulation of RNA binding, control of transcription, DNA repair, protein localization, signal transduction, and recycling of membrane receptors (11). Large-scale proteomic approaches have unraveled a potentially broad range of substrate proteins for PRMT methylation, suggesting a significant role for arginine methylation in cellular processes (13). Moreover, increased methylation of cellular proteins by PRMT may significantly contribute to the level of free methylarginines via protein degradation, as direct methylation of free arginines has not been demonstrated.

Circulating ADMA levels have been assessed in a variety of systemic cardiovascular diseases, and are increased in conditions associated with hypoxia, renal failure, pulmonary hypertension, heart failure, or hypercholesterolemia (10, 14). A recent study by Smith and coworkers demonstrated that pathophysiologic concentrations of ADMA are sufficient to elicit distinct changes in gene expression of coronary endothelial cells, suggesting that increased

(Received in original form March 4, 2006 and in final form April 14, 2006)

This study was supported by grants from the Deutsche Forschungsgemeinschaft (DFG-SFB547) to N.W., F.G., and O.E. and the Alexander von Humboldt Foundation (a Sofja Kovalevskaja Award to O.E. and a Research Fellowship to R.E.M.). D.Z. and K.E.K. were supported by predoctoral fellowships of the International Graduate Program "Molecular Biology and Medicine of the Lung (MBML)."

Correspondence and requests for reprints should be addressed to Oliver Eickelberg, M.D., University of Giessen Lung Center, Department of Medicine II, Aulweg 123, Room 6-11, D-35392 Giessen, Germany. E-mail: oliver.eickelberg@innere.med.uni-giessen.de

Am J Respir Cell Mol Biol Vol 35, pp 436–443, 2006

Originally Published in Press as DOI: 10.1165/rcmb.2006-0097OC on May 11, 2006

Internet address: www.atsjournals.org

extracellular ADMA levels also regulate cellular functions (15). Despite the wealth of information available on circulating plasma ADMA levels, however, no studies have thus far correlated tissue ADMA and PRMT levels. The tissue expression and localization of PRMT isoforms in the lung remains entirely unknown. In this study, we therefore sought to characterize the expression and localization pattern of PRMT isoforms in the lung, and investigated whether PRMT expression and lung ADMA levels changed during exposure to chronic hypoxia.

MATERIALS AND METHODS

Mouse Models

All animal studies were performed according to the guidelines of the University of Giessen and approved by the local authorities (Regierungspräsidentium Giessen, no. II25.3-19c20-15; GI20/10-Nr.22/2000). Male BALB/c mice (20–22 g; Charles River, Sulzfeld, Germany) were exposed to normobaric normoxia ($F_{I_{O_2}}$ of 0.21) or hypoxia ($F_{I_{O_2}}$ of 0.10) in a ventilated chamber system (16). After the indicated times under hypoxic conditions, the lungs were flushed via a catheter in the pulmonary artery with Krebs Henseleit buffer (125 mM NaCl, 4.3 mM KCl, 1.1 mM KH_2PO_4 , 2.4 mM $CaCl_2$, 1.3 mM $MgCl_2$, 23.8 mM $NaHCO_3$, and 13.32 mM glucose, equilibrated with 5.3% CO_2) and pressure-fixed (20 cm H_2O) with 4% (wt/vol) buffered paraformaldehyde in PBS (pH 7.4). Tracheas were ligated and lungs/hearts were excised *en bloc*, submerged in 4% (wt/vol) paraformaldehyde in PBS overnight, and processed for paraffin embedding and sectioning. Lungs were cut into 3- μ m sections and processed as described for immunohistochemistry (17). A separate set of lungs was immediately removed and snap-frozen in liquid nitrogen for RNA and protein extraction. Hematocrit and right heart hypertrophy were measured in all study animals. To measure the ratio of right ventricle wall/left ventricle plus septum (RV/LV+S), the right ventricular walls were trimmed from the left ventricles plus septa, air-dried, and weighed. Similarly, timed pregnant mice were killed at the indicated dates, and pups removed surgically. Lungs were

excised from pups under magnification and immediately processed for further analysis, as described above.

RT-PCR

cDNA was synthesized from total mouse lung RNAs with ImPromII Reverse Transcriptase (Promega, Madison, WI). For PCR amplification of cDNA, 25 μ l reaction mixtures were prepared containing 1 \times PCR Buffer (Invitrogen, Carlsbad, CA), 0.2 mM dNTP mixture (Promega), 1.5 mM $MgCl_2$, specific primers each (0.2 μ M each), 1 U Platinum Taq DNA Polymerase (Invitrogen), and 0.1 μ g of cDNA. PCR products were resolved by 2% (wt/vol) agarose gel electrophoresis and visualized by ethidium bromide staining. In separate experiments, full-length PRMT cDNAs were also cloned into pGEM-T Easy vector (Promega) and identified by restriction digestion and full-length sequencing. For all RT-PCR reactions, the annealing temperature was optimized by gradient PCR in a DNA Engine DYAD Peltier Thermal Cycler (MJ Research, Waltham, MA) over the temperature range 55°C to 65°C. The linear range was determined by running separate PCR reactions at multiple cycle numbers between 18 and 26, to establish entry into the plateau phase. The oligonucleotide primer sequences and optimized cycle number used in all PCR reactions are provided in Table 1.

Western Blot Analysis

Frozen lung tissues were homogenized in lysis buffer (20 mM Tris-Cl [pH 7.5], 150 mM NaCl, 1 mM EDTA, 1 mM EGTA, 1% [wt/vol] Triton-X 100, 2.5 mM sodium pyrophosphate, and 1 mM β -glycerophosphate). The proteinase inhibitor cocktail Complete (Roche Molecular Biochemicals, Indianapolis, IN) and the phosphatase inhibitor Na_3VO_4 (1 mM) were added to the lysis buffer immediately before homogenization. Homogenates were dispersed by multiple aspirations through a 24-gauge needle, agitated at 4°C for 30 min, and centrifuged at 10,000 \times g (4°C) for 10 min. The protein concentrations of tissue lysates were measured using Quick Start Bradford Dye Reagent according to the manufacturer's instructions (Bio-Rad, Hercules, CA). Equal amounts of protein (20 μ g) were separated on 7.5% SDS-PAGE gels and transferred to

TABLE 1. CHARACTERISTICS OF THE PCR ASSAYS DESCRIBED IN THE STUDY

Name	Accession No.	PCR Fragment Size (bp) and (Cycle Number)		PCR Primer Sequence (Sense/Antisense)	Location (nt)
Actin	NM_009608	180	+	5'-cgatatccgcaagacctgt-3'	947-965
		(26)	-	5'-gctggaaggtggacagagag-3'	1,146-1,127
HSC70	NM_031165	450	+	5'-caagcgaagcacaagaagacat-3'	836-860
		(26)	-	5'-ataccaagcgaagaggagtgcac-3'	1,311-1,286
PRMT1	NM_019830	320	+	5'-caccctcacatccgcaactcc-3'	230-252
		(28)	-	5'-cagccactgtcccagcgt-3'	569-550
		1067	+	5'-atggagaattttgtagccacttg-3'	45-68
		(32)	-	5'-tcagcgcacccggtagtcg-3'	1,130-1,112
PRMT2	NM_133182	343	+	5'-cgacaagcaactggggaatac-3'	370-392
		(28)	-	5'-accttctcggcagcaccac-3'	732-713
		1340	+	5'-gaactatggaggcaccaggaga-3'	78-99
		(31)	-	3'-acgccctgttaactgtcacct-3'	1,438-1,418
PRMT3	AK010534	888	+	5'-taaggtgttctggatgttgggtgtgggg-3'	890-917
		(29)	-	5'-catcccggctcactgccctattcc-3'	1,800-1,778
		1660	+	5'-cttggctcggcgccatgtgt-3'	118-137
		(31)	-	5'-catcccggctcactgccctattcc-3'	1,800-1,778
PRMT4	NM_021531	1645	+	5'-cggacctaagatggcagcgg-3'	234-255
		(31)	-	5'-ttcctgtgtctgtcagt-3'	1,895-1,879
		1861	+	5'-taagatggcagcggcgagcag-3'	21-40
		(31)	-	3'-cttgatttggttctcgtgtgtc-3'	1,906-1,882
PRMT5	XM_127802.1	697	+	5'-gagaggagaagatggcggagat-3'	37-65
		(28)	-	5'-aggaaaatgctgtggggagaatggct-3'	760-734
		1918	+	5'-gagaggagaagatggcggcag-3'	37-65
		(29)	-	5'-acactggcagcaggctagaggc-3'	1,981-1,955
PRMT6	BC022889	1147	+	5'-ggggccaacatgtcgtgagcaaga-3'	4-28
		(28)	-	5'-aggtggagggggagaaaaggcaacg-3'	1,175-1,151
PRMT7	AY673972	2108	+	5'-gagccagtggcaccatgaa-3'	116-135
		(32)	-	5'-gcagctgctggccatttat-3'	2,244-2,224

Definition of abbreviations: -, reverse primer used; +, forward primer used; Accession no., GenBank accession number. The table indicates full sequences of all primers used in the RT-PCR assays.

PVDF-PLUS membranes (GE Osmonics Inc., Trevose, PA). Western blots were performed with antibodies against PRMT1 (at a dilution of 1:2,000), PRMT3 (1:2,000), PRMT4 (1:1,000), PRMT5 (1:2,000), PRMT7 (1:1,000), asymmetric dimethylarginine (ASYM24-MDMA; 1:2,000), all from Upstate (Dundee, UK). Anti-PRMT2 (1:1,000) and Anti-PRMT6 (1:500) were obtained from Abcam (Cambridge, UK) and Imgenex (San Diego, CA), respectively. After incubation with secondary antibodies, specific bands were visualized by autoradiography using enhanced chemiluminescence according to the manufacturer's instructions (SuperSignal; Pierce Chemicals, Rockford, IL). Protein expression was normalized to α -tubulin levels detected by anti- α -tubulin (1:2,500, clone B-7; Santa Cruz Biotechnology, Inc., Santa Cruz, CA). Densitometric analysis ($n \geq 6$ for each group) was performed with Quantity One (Bio-Rad) and analyzed using two-tailed Student's *t* test.

Immunohistochemical Analysis

Whole lung sections were deparaffinized in xylene for 3×5 min and rehydrated in 100% ethanol for 2×1 min, 95% ethanol for 2×1 min, and PBS for 1×2 min (17). Antigen retrieval was performed in a pressure cooker using citrate buffer unmasking solution at pH 6.0 (Invitrogen). Immunolocalization for the indicated proteins was detected by AEC staining according to the manufacturer's instructions (Histostain-SP Kits; Invitrogen). Endogenous peroxidase activity was quenched by incubating the sections in 3% (vol/vol) hydrogen peroxide for 2×10 min. Staining specificity was assessed via simultaneous staining of control sections with an unspecific, species-matched primary antibody or preincubation of the primary antibody with blocking peptides where available. Sections were counterstained with hematoxylin for 2 min.

Isolation of Basic Amino Acids from Lung Crude Extracts

Snap-frozen mouse lungs were homogenized in liquid nitrogen, followed by addition of ice-cold lysis buffer (20 mM Tris-Cl [pH 7.5], 150 mM NaCl, 1 mM EDTA, 1 mM EGTA, 1% [vol/vol] Triton X-100, 2 mM Na_3VO_4). Homogenized tissues were incubated for 1 h on ice and centrifuged for 15 min at $10,000 \times g$. Crude extracts were subjected to fractionation on Oasis MCX cation-exchange SPE columns (Waters, Eschborn, Germany). Crude extracts (100 μ l of each sample) were adjusted to a final volume of 1 ml with PBS. All conditioning, washing, and elution steps were performed on a vacuum-manifold with a capacity of 24 columns (Waters) at a flow rate of 0.5 ml/min. The SPE columns were conditioned with 2 ml of methanol/water/ammonia (50:45:5, vol/vol/vol) followed by 2 ml PBS before sample application. Samples were passed through SPE cartridges and contaminating components rinsed off with 2 ml of 0.1 M HCl followed by 2 ml methanol. Basic compounds were eluted with 1 ml of methanol/water/ammonia (50:45:5, vol/vol/vol) and dried under nitrogen stream at 65°C (18).

Derivatization and Chromatographic Separation

Amino acid eluates were redissolved in 230 μ l of distilled water and centrifuged at $10,000 \times g$ for 2 min to remove particulate matter before derivatization for high-performance liquid chromatography (HPLC). The *o*-phthalaldehyde (OPA) was freshly prepared in potassium borate buffer (Grom, Rottenburg-Hailfingen, Germany) according to the manufacturer's instructions. Samples (115 μ l) were then combined with 50 μ l of OPA reagent, immediately transferred to the auto sampler, and injected exactly after 2 min. Quantification of basic amino acids was performed on an HPLC system consisting of an ASI-100 auto sampler, a model P680 gradient pump, a model RF-2000 fluorescence detector, and a data acquisition system (Chromleon 6.60; Dionex, Idstein, Germany). Separation was performed as previously described (18). Fluorescent amino acid derivatives were separated on a SunFire C18 column (4.6×150 mm; 3.5 μ m particle size; 100 \AA pore size) with a μ Bondapak C18 guard column (10 μ M) at 30°C and a flow rate of 1.1 ml/min (all columns were from Waters). After injection of the sample (125 μ l), separation was performed under isocratic conditions with 8.8% (vol/vol) acetonitrile in 25 mM potassium phosphate buffer (pH 6.8) as a solvent. Isocratic conditions were maintained for 30 min. To elute strongly bound compounds, the column was flushed with acetonitrile/water (50:50, vol/vol) for 2 min and re-equilibrated under isocratic conditions for 10 min before the next injection. Fluorescent derivatives were detected at excitation and emission wavelengths of 330 and

450 nm, respectively. L-arginine and ADMA were quantified by two separation steps. For the detection of ADMA, the gain of the detector was switched to a 100-fold higher sensitivity. Calibration was performed on the base of the peak area using six combined standards spanning the range 1.5–450 pmol (60 nM to 18 μ M) for L-Arg, 0.15–45 pmol (6 nM to 1.8 μ M) for ADMA, and 0.09–9 pmol (3.6 nM to 0.36 μ M) for SDMA (all from Sigma, St. Louis, MO) (18).

RESULTS

PRMT Expression in Mouse Lung

We initially characterized full-length PRMT1-7 transcripts by cloning and sequencing full-length cDNAs from adult mouse lung. Mouse PRMT1-6 isoforms have previously been cloned from the mouse; however, our report constitutes the first description of PRMT7 from the mouse. This PRMT7 sequence has been deposited in the GenBank database (accession no. AY673972). Figure 1A demonstrates strong expression of all PRMT isoforms in mouse lung, with no evidence of splice isoforms expressed. All sequences were fully sequenced and shown to be identical to the provisional RefSeq depositions at GenBank. We next analyzed whether lung PRMT levels were regulated during lung development. To do so, mouse lungs were harvested at distinct intervals from E13 to adults and subjected to RT-PCR analysis. As depicted in Figure 1B, PRMT1-7 were abundantly expressed

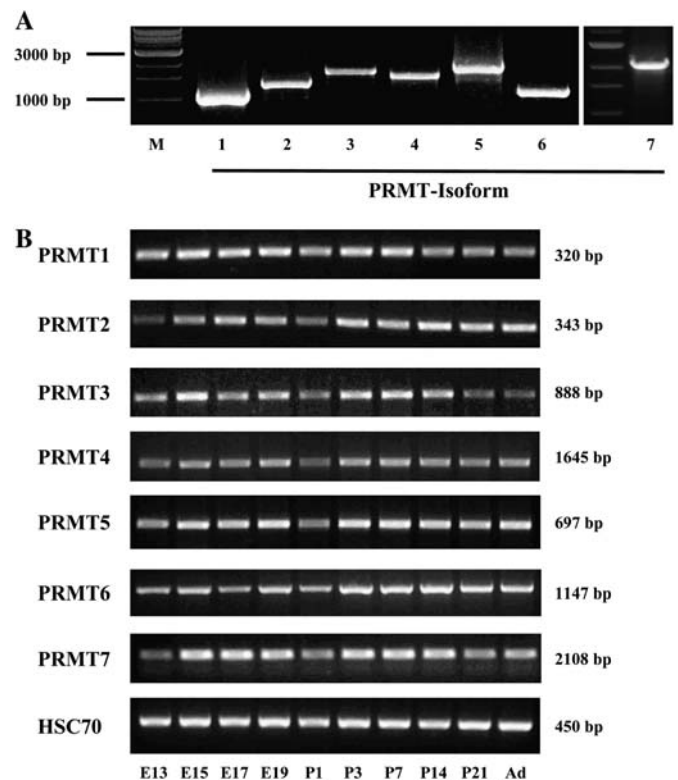


Figure 1. PRMT1-7 expression in adult mouse lung and during lung development. (A) RT-PCR analysis demonstrated the expression of mRNAs encompassing the full-length open reading frame of PRMT1-7 in the adult mouse lung, as indicated below the gel. (B) Semiquantitative RT-PCR analysis demonstrated the expression of PRMT1-7 isoforms during mouse lung development, as indicated below the gel. Panels are representative of the results obtained in at least three independent RT-PCR reactions for every gene. The sizes of the PCR products were approximated by comparison to a molecular mass standard, as indicated on the sides. M, DNA size marker; E, embryonic stage.

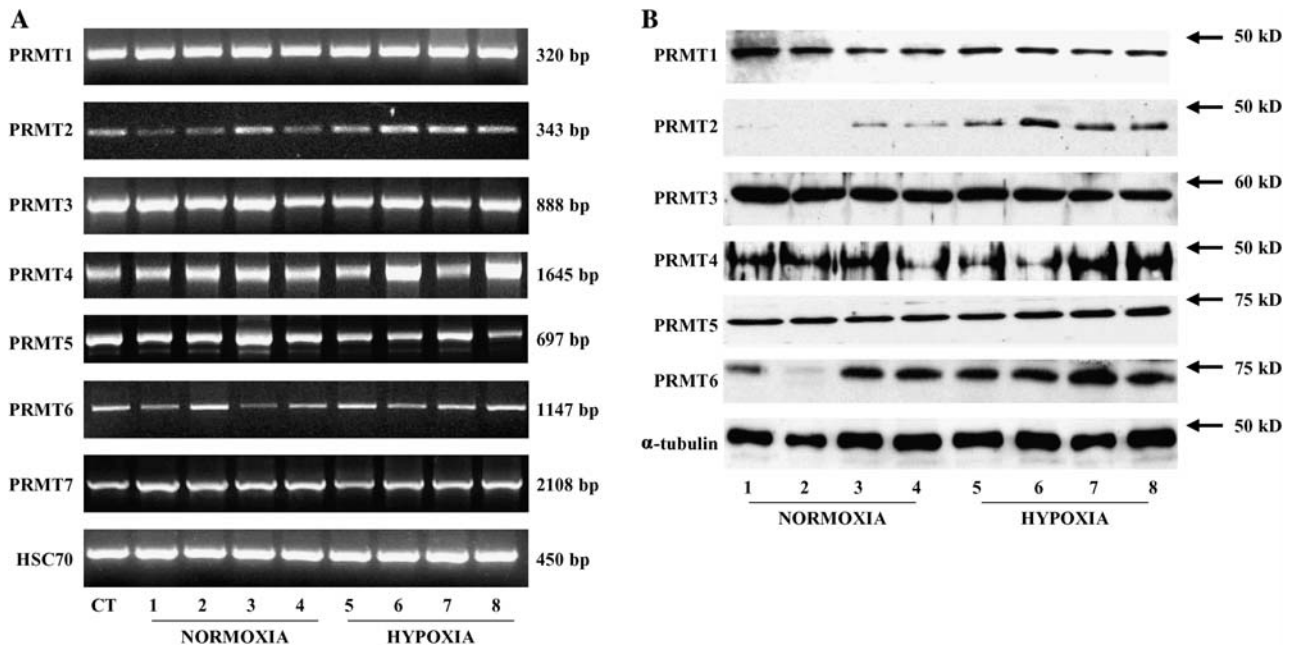


Figure 2. PRMT1-7 expression in mice maintained under normoxia and hypoxia. Mice were kept for up to 3 wk in normobaric normoxia (21% O₂) or hypoxia (10% O₂). Whole lung RNA and protein extractions were then performed and analyzed for PRMT1-7 expression by RT-PCR (A) and Western blot (B), as indicated. The numbers at the base of the panels indicate different mice. (A) As a loading control, RT-PCR for the constitutive heat shock protein 70 (HSC70) was performed. CT, positive RT-PCR control from commercial whole lung RNA. Gels are representative for at least three independent experiments. (B) Whole lung proteins were analyzed for PRMT1-6 expression by Western Blot analyses. Analysis of the constitutive α -tubulin was performed to control for equal loading. Sizes of the specific bands are indicated on the right; gels are representative for at least three independent experiments.

throughout development. While no changes in expression levels were observed in cases of PRMT1, 5, and 7, distinct changes were noted for PRMT2, 3, 4, and 6. While PRMT3 and 4 expression peaked at P7 with a decline thereafter, PRMT2 and 6 expression steadily increased to adulthood (Figure 1B). These data must be cautiously interpreted, however, since mRNA and protein expression levels do not always correlate, as was evident in our hypoxia studies (*see below*).

We then characterized whether PRMT1-6 RNA expression was altered when mice were exposed to 3 wk of chronic normobaric hypoxia (F_IO₂ of 0.10). To ensure proper hypoxic exposure, we determined the ratio of dried right ventricle to left ventricle plus septum (RV/LV+IVS), an indicator of right ventricular hypertrophy secondary to chronic hypoxia-induced pulmonary hypertension. The RV/LV+IVS gradually increased from 0.33 ± 0.02 under normoxia, 0.45 ± 0.01 after 7 d of hypoxia, to 0.48 ± 0.02 after 21 d of hypoxia ($P < 0.005$). Similarly, the hematocrit values increased from 43 ± 0 under normoxia, 53.6 ± 0.6 after 7 d of hypoxia, to 56.6 ± 1.2 after 21 d of hypoxia ($P < 0.01$).

Figure 2 depicts changes in gene expression in lungs of mice exposed to 3 wk of hypoxia, as assessed by RNA and protein analysis. Whereas RNA levels of PRMT1, 3, 4, 5, 6, 7 and the loading control HSC70 did not differ between samples from normoxic and hypoxic mice, PRMT2 RNA levels were upregulated after 3 wk of hypoxia (Figure 2A). As represented in Figure 2B, Western blot analyses revealed an even higher upregulation of PRMT2 protein levels under hypoxia. This effect was specific for PRMT2, as the expression of all other PRMTs investigated did not change significantly in the lungs of hypoxic mice (Figures 2B and 3). To quantify PRMT expression levels, we performed densitometric analyses from at least three different Western blots each. Densitometry indicated a significant difference in

PRMT2 protein expression under hypoxia, whereas we did not observe significant expression differences for all other PRMT isoforms (Figure 3).

PRMT Localization in Mouse Lung

To investigate the cellular localization of PRMT enzymes in the lung in detail, we performed immunohistochemical analyses on lung sections obtained from normoxic and hypoxic animals. Figure 4 depicts representative immunohistochemical stainings

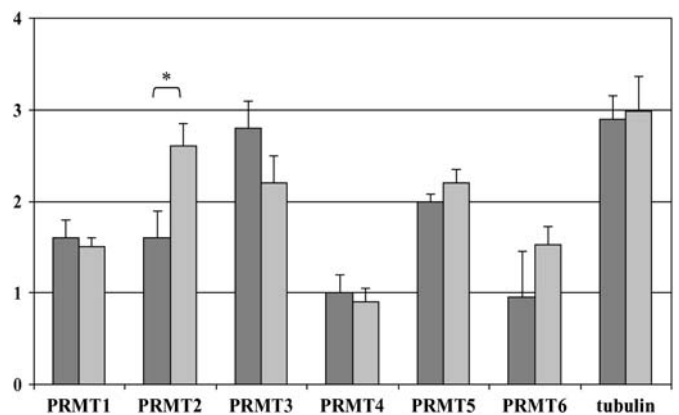


Figure 3. Densitometric analyses of the PRMT protein expression depicted in Figure 2B. Relative expression levels under normoxia and hypoxia were plotted as a ratio of PRMT/ α -tubulin expression for each sample, as indicated ($*P < 0.005$). Solid bars, normoxic samples; shaded bars, hypoxic samples.

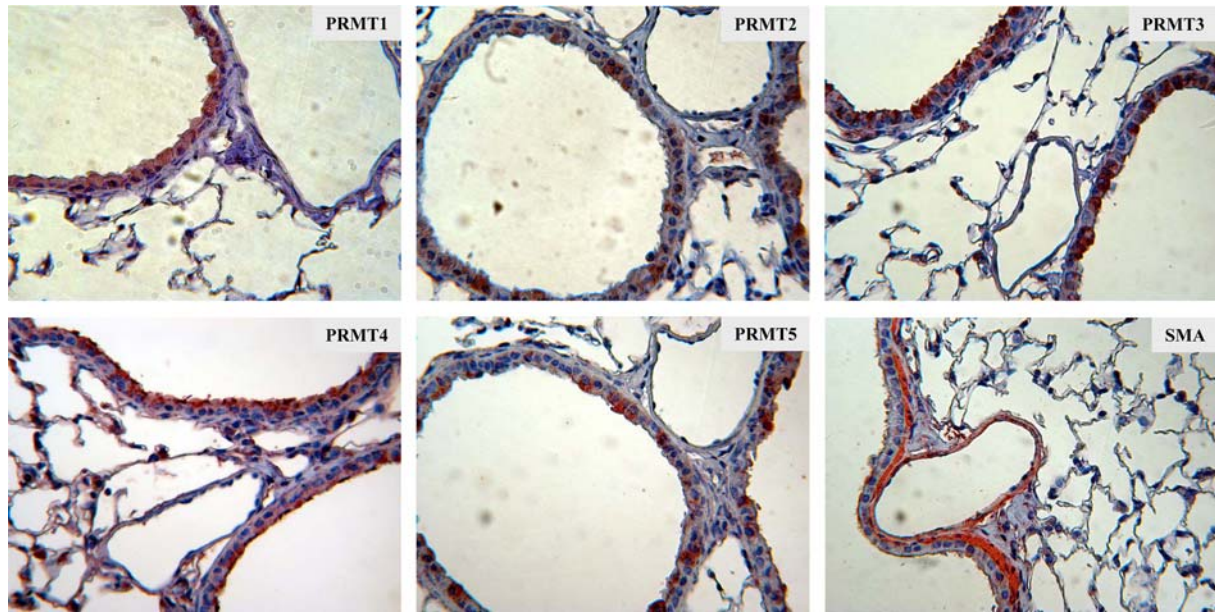


Figure 4. PRMT1-5 immunolocalization in the mouse lung. Lungs from adult normoxic mice were fixed under 20 cm H₂O pressure, processed, and analyzed for PRMT1-5 expression by immunohistochemistry and counterstained with hematoxylin, as indicated. As a positive control, α -smooth muscle actin (SMA) stainings were performed. Data are representative for at least three independent rounds of stainings using at least three different mouse lungs.

demonstrating specific and distinct localization patterns of PRMT1-5 in the mouse lung. PRMT1 exhibited strong homogeneous staining in airway and alveolar type II epithelial cells. PRMT2, 3, and 5 exhibited intermittent staining, and were localized in the cytosol of nonciliated airway epithelial cells and alveolar epithelial cells, but notably absent in vascular smooth muscle and endothelial cells. PRMT4 was present in the apical

part of airway epithelial cells and in alveolar epithelial type II cells (Figure 4). The expression pattern and localization of these isoforms (i.e., PRMT1, 3, 4, and 5) did not differ between lungs derived from normoxic and hypoxic mice (data not shown).

PRMT2 was expressed in the cytosol of some, but not all airway epithelial cells in the lungs of mice exposed to normoxic conditions (Figure 4). In contrast to other PRMT isoforms,

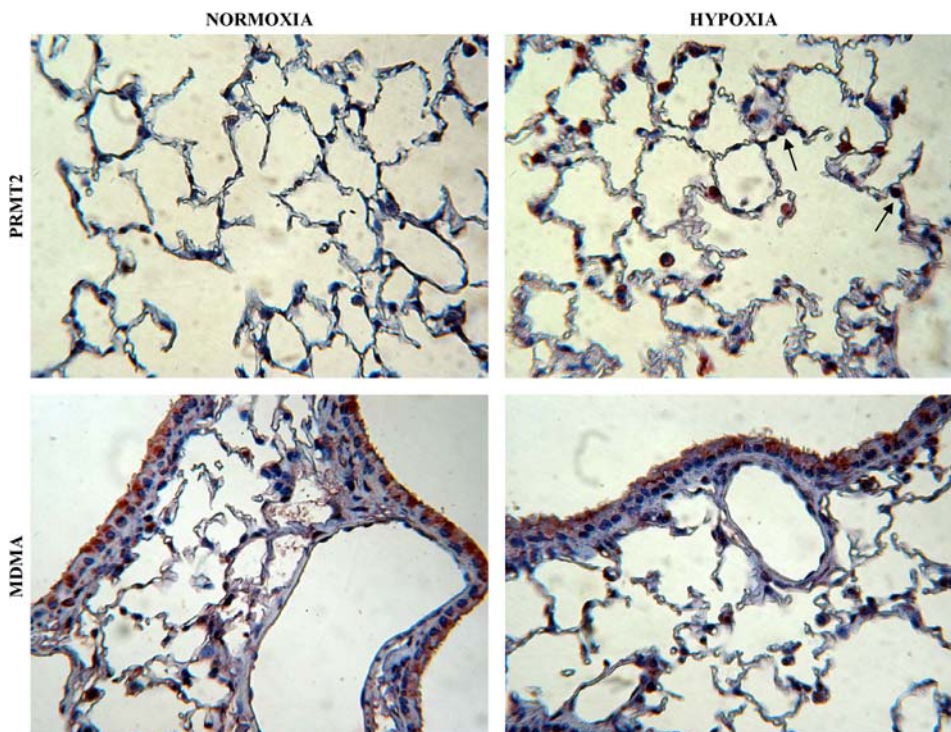


Figure 5. PRMT2 and MDMA staining in normoxic and hypoxic mouse lungs. Lungs were fixed under 20 cm H₂O pressure, processed, and analyzed for PRMT2 and MDMA immunostainings, as indicated. PRMT2 staining is strongly positive in lungs from hypoxic mice, in particular in alveolar type II cells (arrows). Data are representative for at least four independent rounds of stainings using different mouse lungs. MDMA, mono- and dimethylarginine.

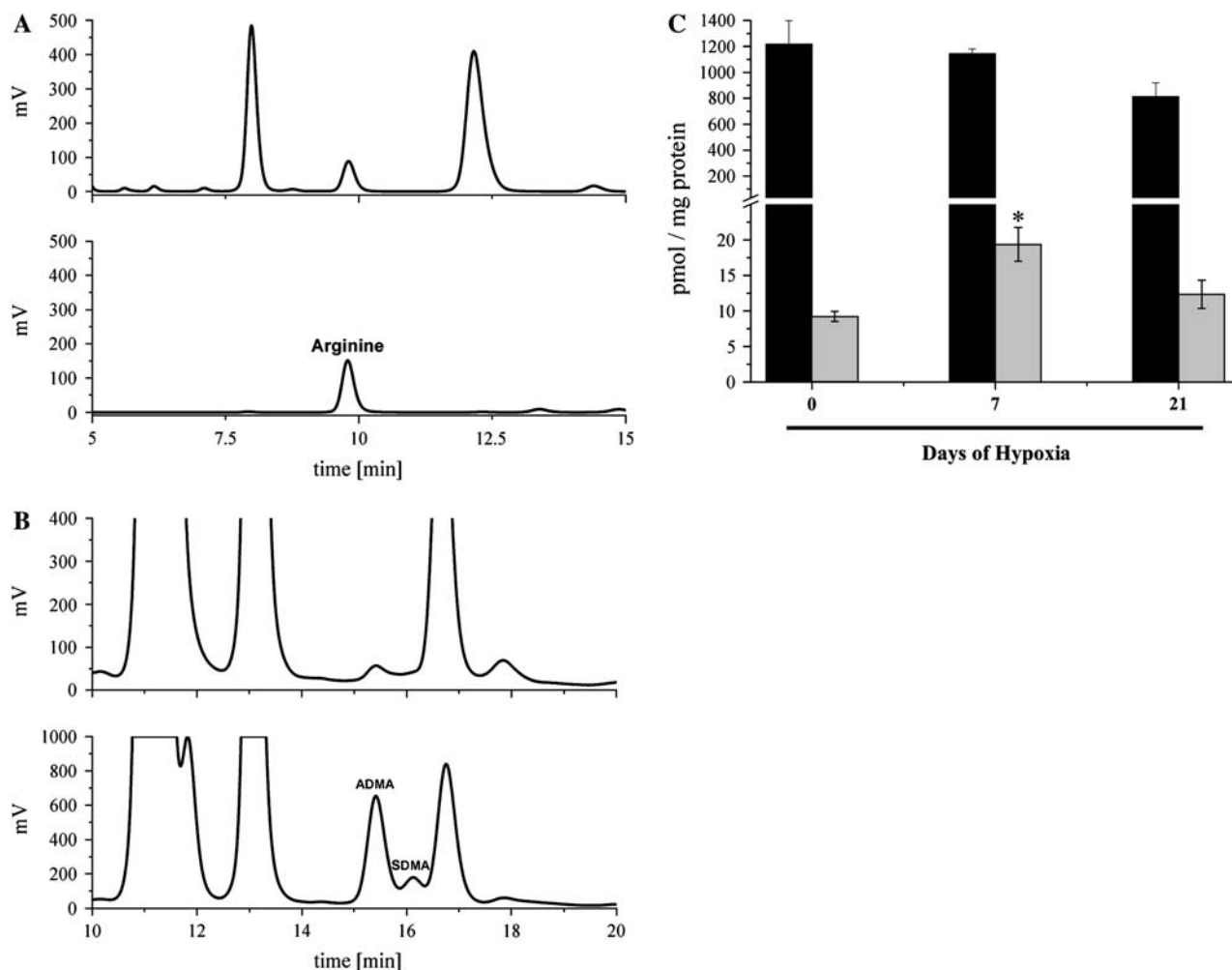


Figure 6. Increased tissue ADMA levels in hypoxic mouse lungs. (A) HPLC chromatograms of the region 5–15 min (upper panel) and standard containing 75 pmol L-arginine (lower panel). (B) HPLC chromatograms of the region 10–20 min (upper panel) from the same sample spiked with 15 pmol of ADMA and 3 pmol of SDMA (lower panel). For the detection of ADMA, the gain of the detector was set to a 100-fold higher sensitivity. Derivatization and chromatographic separation of basic amino acids are described in detail in MATERIALS AND METHODS. (C) Concentrations of arginine (solid bars) and ADMA (shaded bars) in crude lung extracts from mice, maintained under normoxic and hypoxic conditions (Days 7 and 21). Significant differences from normoxic conditions are marked by an asterisk (Student's *t* test, $P < 0.05$).

PRMT2 expression levels changed after hypoxic exposure, where staining became evident in alveolar type II cells and macrophages (Figure 5). The product of PRMT activity, methylated proteins, were also localized to alveolar type II cells and macrophages using an antibody raised against mono- and dimethylated proteins (Figure 5).

Methylated Proteins in Mouse Lung

To analyze whether the end-product of PRMT activity, free cellular ADMA, was also found in the mouse lung, we developed an HPLC-based method to accurately quantify ADMA in crude tissue extracts. Using this protocol, ADMA and arginine were fully separated from other components of lung lysates (Figures 6A and 6B). To confirm the identity of ADMA, crude tissue extract was spiked with ADMA (Figure 6B, lower panel). Taken together, this method permits the simultaneous quantification of arginine and ADMA in crude tissue extracts. As depicted in Figure 6C, hypoxic conditions caused a significant increase in free cellular ADMA levels after 7 d (19.4 ± 2.4 pmol/mg protein versus 9.2 ± 0.7 pmol/mg protein) and a moderate increase after 21 d (12.3 ± 1.9 pmol/mg protein), indicating increased PRMT activity. Interestingly, we also observed a slight reduction in free

arginine (813 ± 107 pmol/mg protein versus $1,219 \pm 180$ pmol/mg protein) after 21 d, while arginine levels after 7 d did not change significantly (Figure 6C). In conclusion, lung ADMA levels and ADMA/arginine ratios were increased under hypoxic conditions (Table 2).

DISCUSSION

The key observations of this study are that (1) PRMT isoforms are expressed at the mRNA and protein levels in the mouse

TABLE 2. COMPARISON OF THE DEGREE OF ASYMMETRICAL ARGININE DIMETHYLATION (ARGININE AND ADMA) IN CRUDE LUNG EXTRACTS FROM MICE MAINTAINED UNDER NORMOXIC AND HYPOXIC CONDITIONS (7 AND 21 d)

	Arginine (pmol/mg protein)	ADMA (pmol/mg protein)	Arginine/ADMA ratio
Normoxia	1,219 ± 180	9.2 ± 0.7	133 ± 30
Hypoxia 7d	1,146 ± 36	19.4 ± 2.4	60 ± 7
Hypoxia 21d	813 ± 107	12.3 ± 1.9	68 ± 18

Data are represented as mean ± SD ($n = 3$).

lung, and are localized predominantly in airway and alveolar type II epithelial cells; (2) PRMT2 expression is selectively upregulated in alveolar epithelial cells in response to chronic hypoxia; and (3) increased PRMT2 expression coincides with increased tissue ADMA levels and decreased L-Arg/ADMA ratios in hypoxic mouse lungs. These data thus support an important role for PRMT enzymes in the lung, and suggest an as yet unappreciated role for PRMT-mediated ADMA generation in pulmonary homeostasis and hypoxia-induced changes in lung epithelial cells.

PRMTs are the only group of enzymes known to methylate arginine residues in select target proteins, which thus far remains the only known function of PRMTs (11, 19). In this study, we could show that all PRMT isoforms are expressed in the mouse lung by RT-PCR, Western blot, and immunohistochemical analysis. We were able to detect full-length mRNAs corresponding to the entire open reading frames of PRMT1-7 by RT-PCR, with corresponding protein expression patterns for PRMT1-6. Although three splice variants have been described for PRMT1 (20) and four splice variants have been described for PRMT4 (21), no evidence of alternative splicing was observed in the mouse lung (Figure 1). We were unable to detect PRMT7 protein expression, as we were lacking suitable antibodies for detection by Western Blot or immunohistochemistry, respectively. However, our report constitutes the first report of PRMT7 in the mouse. Much to our interest, PRMT isoforms were expressed in the bronchial and alveolar epithelium, suggesting an important role for PRMT function in this pulmonary compartment.

We detected a significant increase in PRMT2 mRNA and protein expression in animals subjected to 3 wk of chronic hypoxia, which coincided with increased protein methylation in lung homogenates. Assuming constant protein turnover, this would be expected to lead to increased ADMA concentrations under hypoxia, which has indeed been demonstrated previously in hypoxic lungs (22). In a recent study, Millatt and coworkers demonstrated increased lung ADMA levels in hypoxic rat lungs, which coincided with decreased dimethylarginine dimethylaminohydrolase (DDAH) I expression and activity (22). DDAH I and II are the enzymes responsible for ADMA degradation. In addition, chronic hypoxia also leads to decreased expression of the second known ADMA-metabolizing enzyme DDAH II in pig lungs (23), thus confirming the observation that hypoxia affects lung ADMA levels via dual regulation of the PRMT-ADMA-DDAH axis: it increases PRMT expression and concomitantly decreases DDAH expression, thus leading to a synergistic overall accumulation of ADMA concentrations.

Interestingly, PRMT and DDAH isoforms both localize to bronchial epithelial cells, suggesting a physiologic role for these enzymes in lung epithelial homeostasis. While PRMTs in vascular smooth muscle have been suggested to be part of the systemic arginine-ADMA metabolism (10), the role of PRMT expression in bronchial and alveolar epithelial cells is intriguing and remains to be elucidated. Since ADMA can act as an endogenous inhibitor of NOS enzymes, a system of crucial importance for the alveolar-endothelial crosstalk, PRMT in bronchial and alveolar epithelial cells may represent an important local regulatory system for NO release and activity in the lung.

A synergistic effect of hypoxia on PRMT, DDAH, and NOS activity in the lung is suggested to lead to increased vasoconstriction and vascular remodeling (22–25). PRMT activity may thus be directly linked to the NO system by ADMA generation. Pathophysiologic roles for ADMA as an endogenous NOS inhibitor have indeed been suggested in several cardiovascular diseases, including atherosclerosis, hypertension, or diabetes (26–32). It is highly unlikely, however, that such a complex system (i.e., the evolution of seven divergent PRMT isoforms) merely

serves to generate a chemically rather simple byproduct (i.e., ADMA or SDMA). In this respect, the PRMT system probably serves additional roles that remain elusive. Several investigators have suggested that the post-translational modification of target proteins by PRMT arginine methylation modulates protein function (19, 33–36). Among the proteins identified thus far are RNA-binding proteins, such as Sam68 (37), and proteins involved in signal transduction, such as STAT-1 (38), STAT-6 (39), or the EWS protein (40). The time course and target arginine residues in these examples have been well described, but relatively little is known about the effects of methylation on protein function. Furthermore, no substrate of PRMT2 has been described to date, although several molecules with proposed roles in tissue remodeling and respiratory physiology are known to form complexes with PRMT2, including estrogen receptor α , retinoic acid receptor α , and peroxisome proliferator-activated receptor γ , which have proposed roles in tissue remodeling and respiratory physiology (41). In this respect, the high expression levels of PRMT isoforms in the lung observed in our studies may indicate an as yet uncharacterized function in pulmonary physiology and pathophysiology. Selective manipulation of PRMT expression or activity in the lung may therefore serve as a valuable tool to uncover novel physiologic and pathophysiologic roles of PRMT biology.

Conflict of Interest Statement: None of the authors has a financial relationship with a commercial entity that has an interest in the subject of this manuscript.

Acknowledgments: The authors are indebted to Werner Seeger, M.D., for critical reading of the manuscript, and to all members of the Eickelberg Lab for valuable discussions.

References

1. Stenmark KR, Bouchez D, Nemenoff R, Dempsey EC, Das M. Hypoxia-induced pulmonary vascular remodeling: contribution of the adventitial fibroblasts. *Physiol Res* 2000;49:503–517.
2. Stenmark KR, Gerasimovskaya E, Nemenoff RA, Das M. Hypoxic activation of adventitial fibroblasts: role in vascular remodeling. *Chest* 2002;122:326S–334S.
3. Zaiman A, Fijalkowska I, Hassoun PM, Tudor RM. One hundred years of research in the pathogenesis of pulmonary hypertension. *Am J Respir Cell Mol Biol* 2005;33:425–431.
4. Meyrick B, Reid L. Normal postnatal development of the media of the rat hilar pulmonary artery and its remodeling by chronic hypoxia. *Lab Invest* 1982;46:505–514.
5. Meyrick B, Reid L. The effect of continued hypoxia on rat pulmonary arterial circulation: an ultrastructural study. *Lab Invest* 1978;38:188–200.
6. Le Cras TD, McMurtry IF. Nitric oxide production in the hypoxic lung. *Am J Physiol Lung Cell Mol Physiol* 2001;280:L575–L582.
7. Hoepfer MM, Rubin LJ. Update in pulmonary hypertension 2005. *Am J Respir Crit Care Med* 2006;173:499–505.
8. Leiper J, Vallance P. Biological significance of endogenous methylarginines that inhibit nitric oxide synthases. *Cardiovasc Res* 1999;43:542–548.
9. Leiper JM. The DDAH-ADMA-NOS pathway. *Ther Drug Monit* 2005;27:744–746.
10. Vallance P, Leiper J. Cardiovascular biology of the asymmetric dimethylarginine:dimethylarginine dimethylaminohydrolase pathway. *Arterioscler Thromb Vasc Biol* 2004;24:1023–1030.
11. Lee DY, Teyssier C, Strahl BD, Stallcup MR. Role of protein methylation in regulation of transcription. *Endocr Rev* 2005;26:147–170.
12. Leiper JM, Vallance P. The synthesis and metabolism of asymmetric dimethylarginine (ADMA). *Eur J Clin Pharmacol* 2006;62:33–38.
13. Ong SE, Mittler G, Mann M. Identifying and quantifying in vivo methylation sites by heavy methyl SILAC. *Nat Methods* 2004;1:119–126.
14. Boger RH, Cooke JP, Vallance P. ADMA: an emerging cardiovascular risk factor. *Vasc Med* 2005;10:S1–S2.
15. Smith CL, Anthony S, Hubank M, Leiper JM, Vallance P. Effects of ADMA upon gene expression: an insight into the pathophysiological significance of raised plasma ADMA. *PLoS Med* 2005;2:e264.
16. Weissmann N, Zeller S, Schafer RU, Turowski C, Ay M, Quanz K, Ghofrani HA, Schermuly RT, Fink L, Seeger W, et al. Impact of

- mitochondria and NADPH oxidases on acute and sustained hypoxic pulmonary vasoconstriction. *Am J Respir Cell Mol Biol* 2005;34:505–513.
17. Vicencio AG, Lee CG, Cho SJ, Eickelberg O, Chuu Y, Haddad GG, Elias JA. Conditional overexpression of bioactive transforming growth factor-beta1 in neonatal mouse lung: a new model for bronchopulmonary dysplasia? *Am J Respir Cell Mol Biol* 2004;31:650–656.
 18. Bulau P, Zakrzewicz D, Kitowska K, Wardega B, Kreuder J, Eickelberg O. Quantitative assessment of arginine methylation in free versus protein-incorporated amino acids in vitro and in vivo using protein hydrolysis and high-performance liquid chromatography. *Biotechniques* 2006;40:305–310.
 19. McBride AE, Silver PA. State of the arg: protein methylation at arginine comes of age. *Cell* 2001;106:5–8.
 20. Scorilas A, Black MH, Talieri M, Diamandis EP. Genomic organization, physical mapping, and expression analysis of the human protein arginine methyltransferase 1 gene. *Biochem Biophys Res Commun* 2000;278:349–359.
 21. Ohkura N, Takahashi M, Yaguchi H, Nagamura Y, Tsukada T. Coactivator-associated arginine methyltransferase 1, CARM1, affects pre-mRNA splicing in an isoform-specific manner. *J Biol Chem* 2005;280:28927–28935.
 22. Millatt LJ, Whitley GS, Li D, Leiper JM, Siragy HM, Carey RM, Johns RA. Evidence for dysregulation of dimethylarginine dimethylaminohydrolase I in chronic hypoxia-induced pulmonary hypertension. *Circulation* 2003;108:1493–1498.
 23. Arrigoni FI, Vallance P, Haworth SG, Leiper JM. Metabolism of asymmetric dimethylarginines is regulated in the lung developmentally and with pulmonary hypertension induced by hypobaric hypoxia. *Circulation* 2003;107:1195–1201.
 24. Weissmann N, Nollen M, Gerigk B, Ardeschir Ghofrani H, Schermuly RT, Gunther A, Quanz K, Fink L, Hanze J, Rose F, et al. Downregulation of hypoxic vasoconstriction by chronic hypoxia in rabbits: effects of nitric oxide. *Am J Physiol Heart Circ Physiol* 2003;284:H931–H938.
 25. Shirai M, Pearson JT, Shimouchi A, Nagaya N, Tsuchimochi H, Ninomiya I, Mori H. Changes in functional and histological distributions of nitric oxide synthase caused by chronic hypoxia in rat small pulmonary arteries. *Br J Pharmacol* 2003;139:899–910.
 26. Cooke JP. Does ADMA cause endothelial dysfunction? *Arterioscler Thromb Vasc Biol* 2000;20:2032–2037.
 27. Cooke JP. ADMA: its role in vascular disease. *Vasc Med* 2005;10:S11–S17.
 28. Boger RH, Bode-Boger SM, Szuba A, Tsao PS, Chan JR, Tangphao O, Blaschke TF, Cooke JP. Asymmetric dimethylarginine (ADMA): a novel risk factor for endothelial dysfunction: its role in hypercholesterolemia. *Circulation* 1998;98:1842–1847.
 29. Kielstein JT, Bode-Boger SM, Hesse G, Martens-Lobenhoffer J, Takacs A, Fliser D, Hoepfer MM. Asymmetrical dimethylarginine in idiopathic pulmonary arterial hypertension. *Arterioscler Thromb Vasc Biol* 2005;25:1414–1418.
 30. Weis M, Kledal TN, Lin KY, Panchal SN, Gao SZ, Valantine HA, Mocarski ES, Cooke JP. Cytomegalovirus infection impairs the nitric oxide synthase pathway: role of asymmetric dimethylarginine in transplant arteriosclerosis. *Circulation* 2004;109:500–505.
 31. Stuhlinger MC, Oka RK, Graf EE, Schmolzer I, Upson BM, Kapoor O, Szuba A, Malinow MR, Wascher TC, Pachinger O, et al. Endothelial dysfunction induced by hyperhomocyst(e)inemia: role of asymmetric dimethylarginine. *Circulation* 2003;108:933–938.
 32. Stuhlinger MC, Stanger O. Asymmetric dimethyl-L-arginine (ADMA): a possible link between homocyst(e)ine and endothelial dysfunction. *Curr Drug Metab* 2005;6:3–14.
 33. Yadav N, Lee J, Kim J, Shen J, Hu MC, Aldaz CM, Bedford MT. Specific protein methylation defects and gene expression perturbations in coactivator-associated arginine methyltransferase 1-deficient mice. *Proc Natl Acad Sci USA* 2003;100:6464–6468.
 34. Tang J, Frankel A, Cook RJ, Kim S, Paik WK, Williams KR, Clarke S, Herschman HR. PRMT1 is the predominant type I protein arginine methyltransferase in mammalian cells. *J Biol Chem* 2000;275:7723–7730.
 35. Lin CH, Huang HM, Hsieh M, Pollard KM, Li C. Arginine methylation of recombinant murine fibrillar by protein arginine methyltransferase. *J Protein Chem* 2002;21:447–453.
 36. Mowen KA, David M. Analysis of protein arginine methylation and protein arginine-methyltransferase activity. *Sci STKE* 2001;2001:PL1.
 37. Cote J, Boisvert FM, Boulanger MC, Bedford MT, Richard S. Sam68 RNA binding protein is an in vivo substrate for protein arginine N-methyltransferase 1. *Mol Biol Cell* 2003;14:274–287.
 38. Mowen KA, Tang J, Zhu W, Schurter BT, Shuai K, Herschman HR, David M. Arginine methylation of STAT1 modulates IFNalpha/beta-induced transcription. *Cell* 2001;104:731–741.
 39. Chen W, Daines MO, Hershey GK. Methylation of STAT6 modulates STAT6 phosphorylation, nuclear translocation, and DNA-binding activity. *J Immunol* 2004;172:6744–6750.
 40. Belyanskaya LL, Gehrig PM, Gehring H. Exposure on cell surface and extensive arginine methylation of ewing sarcoma (EWS) protein. *J Biol Chem* 2001;276:18681–18687.
 41. Qi C, Chang J, Zhu Y, Yeldandi AV, Rao SM, Zhu YJ. Identification of protein arginine methyltransferase 2 as a coactivator for estrogen receptor alpha. *J Biol Chem* 2002;277:28624–28630.